Article

Local Climate Zones to Identify Urban Surface Heat Islands: a Systematic Review

Rodrigo Fernandes [1], Victor Nascimento [1,2], Marcos Freitas [1], Jean Ometto [3]

[1] Postgraduate Program in Remote Sensing (PPGSR), University of Rio Grande do Sul (UFRGS), Brazil; rodrigopassosufrgs@gmail.com (R.F.); mfreitas@ufrgs.br (M.F.)
[2] Engineering, Modelling and Applied Social Sciences Center, Federal University of ABC (UFABC), Brazil; victor.fernadez@ufabc.edu.br (V.F.)
[3] Earth System Science Center, National Institute for Space Research (INPE), Brazil; jean.ometto@inpe.br (J.O.)
* Correspondence: rodrigopassosufrgs@gmail.com

Abstract: The Land Surface Temperature (LST) is an essential indicator for analyzing the Surface Urban Heat Island (SUHI). A factor contributing to its occurrence is the reflections of the different materials in urban and rural areas, which significantly affect the energy balance near the surface. Therefore, recent studies have increasingly used the Local Climate Zones (LCZ) classification system to discriminate those urban areas. Therefore, our study aims to do a systematic review using the PRISMA method of LCZ classification applied to understand the LST and the SUHI phenomenon. At first, it was found in the scientific literature 10,403 articles which, after passing through filtering stages, resulted in 51 that were further analyzed. Our results showed that these articles were very recent, beginning in 2016. However, presenting an increasing trend. China was the country with more studies. Landsat and TERRA/AQUA sensors appeared in 82% of the studies. The method that appears the most to LCZ definitions is from the World Urban Database. Finally, considering the current climatic changes, this systematic review can help new studies on SUHI identification through LCZ in different world areas using remote sensing data to estimate the LST.

Keywords: SUHI; LST; LCZ; PRISMA; VosViewer

1. Introduction

Cities have been the main human settlements in the world since 2007 when they overtook rural regions. Nowadays, about 55% of the population currently lives in urban areas, and it is expected to reach 68% in 2050 [1]. This increase in urbanization causes urban climate problems. One of the best known is the Urban Heat Island (UHI) phenomenon, referred to in the literature as the increase in the city's center temperature concerning their rural surroundings.

According to [2], there are three UHI types: i) The Canopy Layer Urban Heat Island (CLUHI), 2) The Urban Boundary Layer (UBL), and 3) The Surface Urban Heat Island (SUHI). This last one was considered in this study. This phenomenon is critical because it disturbs the urban system, which is more enhanced by climate change, affecting the population psychologically and physiologically. In addition, it also impacts economic activities, morbidity and mortality increases, energy consumption, and violent behaviors [3].

The SUHI can be obtained using several Land Surface Temperature (LST) remote sensing data. The LST is an important indicator to measure the SUHI phenomenon since it measures the energy balance near the surface, affecting the surface heat distribution process, which significantly alters the urban climate [4].

As a result, the land urbanization effects in SUHI are well discussed in Land Use and Cover (LULC) maps. In this context, a new LULC classification system called Local

Preprints (www.preprints.org) | NOT PEER-REVIEWED | Posted: 15 December 2022 doi:10.20944/preprints202212.0260.v1

Climate Zones (LCZ) arranges the different urban and rural areas in more detail. In addition, the LCZ has been increasingly used in urban heat islands studies [5]. It was initially proposed in 2012 when regional climate zones were divided into several local climate zones within cities according to different LULC surface types, consequently allowing the correlation between climate information and urban planning [6]. The LCZ classification system consists of two main categories, the built and the land cover type, based on building density shape geometry and surface characteristics, including 17 subcategories, as seen in Figure 1.

Therefore, the scientific literature that uses the Local Climate Zones classification to study the Land Surface Temperature and the Surface Urban Heat Island phenomenon was systematically reviewed in this study to follow the state of the art of this scientific theme, organizing sensors and methods most used, and the regional/global contributions, among others.

Figure 1. LCZ classification scheme. Source: [7].

Preprints (www.preprints.org) | NOT PEER-REVIEWED | Posted: 15 December 2022 doi:10.20944/preprints202212.0260.v1

2. Materials and Methods

Few studies make a systematic review to understand the Local Climate Zones application to analyze Urban Heat Islands, such as [8-10]. However, these studies do not focus on the Surface Urban Heat Islands. Therefore, a systematic review was conducted using the Preferred Reporting Items for Systematic Reviews (PRISMA) method to identify the remote sensing research trends applied to Surface Urban Heat Islands identification considering the LCZ classification. Each review step was described in more detail and synthesized in the flowchart shown in Figure 2.

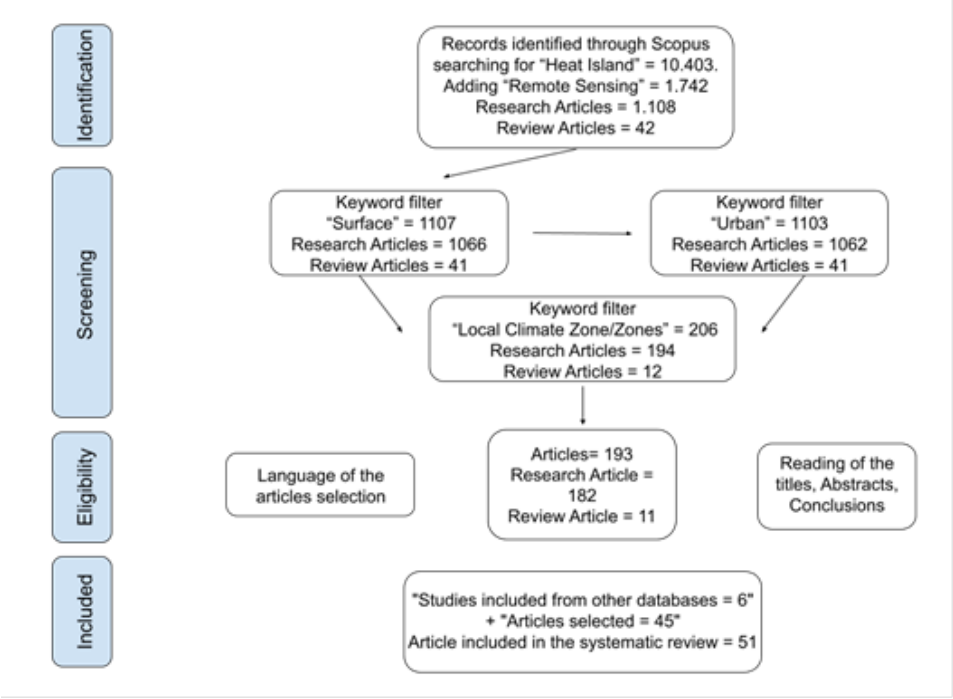

Figure 2. PRISMA flowchart of the phases of the research methodology.

2.1. Step 1: Identification

In the identification phase, the approach adopted for consulting the literature consisted of a search for words that best represented the subject of interest. The keywords were used to filter the Scopus library (www.scopus.com), one of the world's most extensive peer-reviewed scientific literature databases [11]. Using "heat island," 10,403 articles were found in this first step. However, after using the "remote sensing" keyword, 1,174 documents remained. Of these, 1108 were research articles, and 42 were review articles.

2.2. Step 2: Selection

The articles found in the previous step were subsequently extracted to the selection stage. The keywords "Surface" and "Urban" were applied through a filtering tool, but it did not almost reduce the number of articles found. Then, they were passed through a new filter using the keyword "local climate zone/zones," and the number of articles was significantly reduced to 206. Of these, 194 were research articles, and 12 were review articles.

2.3. Step 3: Eligibility

For the eligibility step, it is essential to highlight that only research and review articles in Portuguese or English were chosen. In addition, titles, abstracts, and conclusions of these 206 documents were read and selected only the ones whose content was directly

Preprints (www.preprints.org) | NOT PEER-REVIEWED | Posted: 15 December 2022 doi:10.20944/preprints202212.0260.v1

related to surface urban heat islands using remote sensing data within the local climate zones LULC classification.

2.4. Step 4: Inclusion

In this final step, inclusion, 45 articles were selected, none being review articles. In addition, six articles cited by the articles read and found in databases other than Scopus were added to the analysis. Therefore, 51 articles were included in this systematic review and had their information cataloged.

2.5. Step 5: Data analysis

All the articles selected in the inclusion stage were read and had their information cataloged. Some aspects considered were: (i) scientific production relevance, (ii) regional and global contribution, (iii) satellites and sensors used, as well as their frequency, (iv) methods used to obtain the land surface temperature (LST), (v) methods used to identify the surface urban heat island (SUHI), (vi) methods used to obtain the local climate zones (LCZ), (vii) variables associated with SUHI and LCZ, and (viii) the most frequent software used. In addition, the VosViewer was used to identify the article's reviewed relevance, regional and global contributions, main keywords used, year of publication, and trends among the authors.

3. Results and Discussion

This section is divided into subheadings to provide an organized, concise, and precise description of the results and their interpretation and discussion.

3.1. Relevance of Scientific Production

Of the 10,403 articles found in the scientific literature Scopus database, during the applications of the filters shown in Figure 01, only 51 articles remained to be analyzed in more detail. These reviewed articles were published between 2016 and 2022 (Figure 3), The oldest one was published in September 2016, and the most recent was in June 2022, the month in which the data were collected.

Figure 3. Distribution of publications from September 2016 to June 2022.

Excluding the year 2017 from the period because there was no publication on the subject, we noticed a growing trend in publications beginning in 2019, with nine

 doi:10.20944/preprints202212.0260.v1

publications this year. The most prominent years were the most recent ones, 2020 and 2021, with 12 and 18 publications, respectively. Quite possibly, the last year of analysis, 2022, can easily exceed the previous ones since nine publications were found in the literature related to the subject studied only in the first semester. It is worth highlighting that the LCZs was only created in 2012 [6]. In addition, their approach focused only on Atmospheric Urban Heat Islands, explaining why publications on local climate zones related to surface urban heat islands began to appear only in 2016.

In addition to the publications distributions analysis, each article's citations were counted, thus serving to evaluate its influence. However, even if they are all recent, a normalization was used to adjust their citation number over time and define their influence using (Equation 1).

$$\text{Influence} = \textit{Citations}/(\textit{Year basis} - \textit{Year of publication}) \quad (1)$$

Where, *Citations* are the article citations number; *Year basis* is the year that the systematic review is being done, in this case, 2022; and *Year of publication* is the year in which the article was published.

Therefore, after applying this Equation, the articles were ranked from most to least influential, and the six most influential found in this systematic review are presented in Table 1. Furthermore, all the other articles reviewed are presented in chronological order in supplementary Table A1.

Table 1. Most influential articles.

Title	Year	Journal	Influence	Author
Optimizing local climate zones to mitigate urban heat island effect in human settlements	2020	Journal of Cleaner Production	49.5	[4]
Spatial variability and temporal heterogeneity of surface urban heat island patterns and the suitability of local climate zones for land surface temperature characterization	2021	Remote Sensing	37	[12]
Analyses of land surface temperature (LST) variability among local climate zones (LCZs) comparing Landsat-8 and ENVI-met model data	2021	Sustainable Cities and Society	19	[13]
Evaluation of urban heat islands using local climate zones and the influence of sea-land breeze	2020	Sustainable Cities and Society	17.5	[14]
Detecting multi-temporal land cover change and land surface temperature in Pearl River Delta by adopting local climate zone	2019	Urban Climate	14.6	[15]

Preprints (www.preprints.org) | NOT PEER-REVIEWED | Posted: 15 December 2022 doi:10.20944/preprints202212.0260.v1

Understanding Land Surface Temperature Differences of Local Climate Zones Based on Airborne Remote Sensing Data	2018	IEEE Journal of Selected Topics in Applied Earth Observations and Remote Sensing	11.5	[16]

Among the most influential articles, some things in common are the regional scale study area and the Landsat sensors used in their research. Except for [16], which used hyperspectral and thermal data aided by Light Detection and Ranging (LIDAR) to identify vegetation, constructions, soil, and water surfaces.

The most influential article tries to mitigate urban heat island effects [4]. In this study, the authors identified human settlement in a city in China. They analyzed the different LCZ classes' thermal characteristics to alleviate the SUHI effect and improve the citizens' quality of life. However, although this article is the most influential one, the author did not present a good connection between the authors reviewed, considering the cluster produced using the VosViewer software shown in Figure 4.

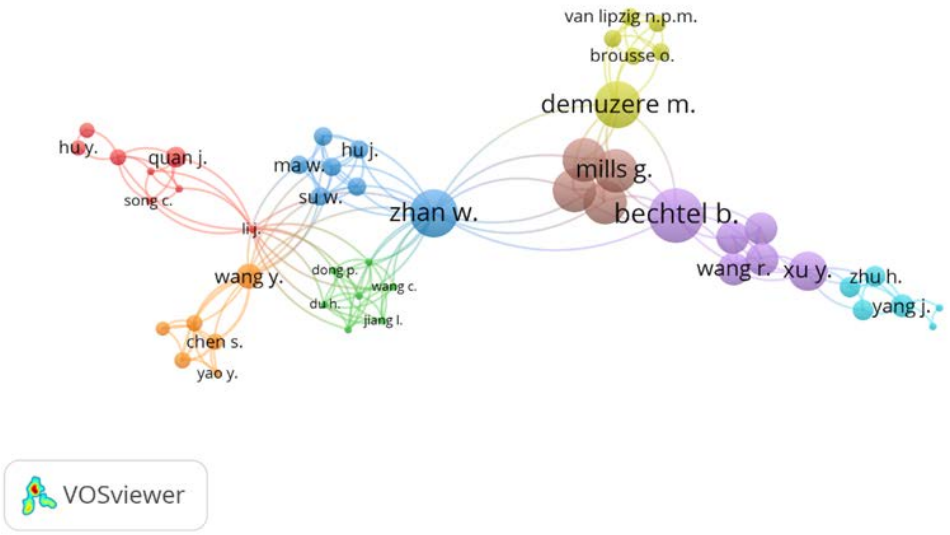

Figure 4. Author's maps by citation.

3.2. Regional and Global Contribution

The connection between the country's collaboration network using VosViewer is presented in Figure 5 and Table 2.

Preprints (www.preprints.org) | NOT PEER-REVIEWED | Posted: 15 December 2022 doi:10.20944/preprints202212.0260.v1

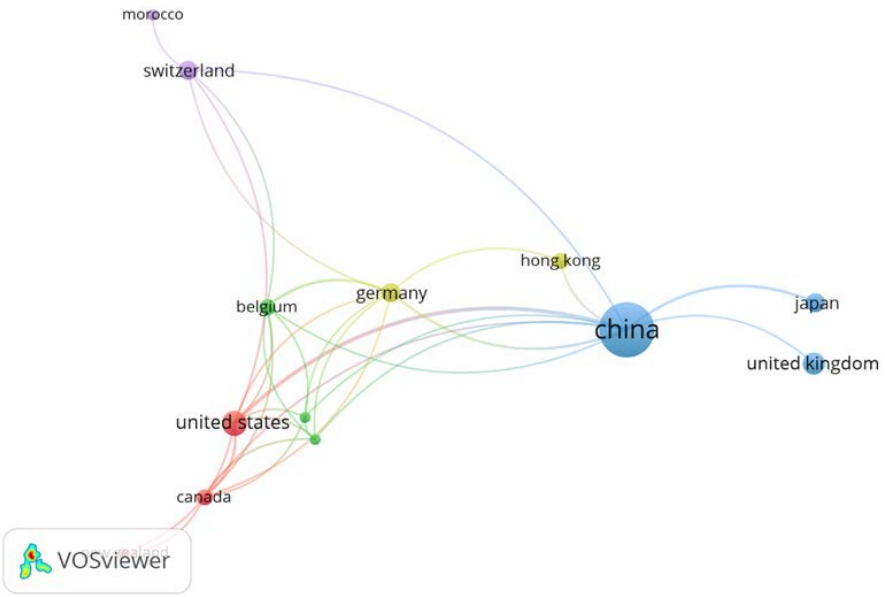

Figure 5. Cluster network analysis of the principal connections among the author's countries of the reviewed articles.

The connection network among the author's countries has 13 nodes, 5 *clusters,* and 32 links. The link has a force and is represented by a positive numerical value; the higher the value, the stronger the power will be. Indicating, for example, the number of cited references that two nodes have in common, publications in which the authors are co-authors, or even the number of publications in which two terms coincide [17].

Also, with VosViewer, the author's country institutions origin in Table 2 were assessed.

Table 2. Originating countries of the reviewed article's author's institutions.

Countries	Documents	Citations	Strength
China	24	337	82
United States (US)	5	123	31
United Kingdom	4	71	45
Serbia	3	82	17
Japan	3	61	23
Switzerland	3	40	8
Belgium	2	100	18

It is noticed that the highest contribution comes from China, with 48% of the articles and approximately 33% of the citations, followed by the US, with 10% of the articles and about 12% of the quotation. In the third place, the United Kingdom obtained a greater strength, even with one article less than the US. This fact may occur by the connections between the authors of the respective countries with China. In addition, the other countries have less than four articles each, with strength below the average.

3.3. Analysis of Satellites and Sensors

In the articles reviewed, several sensors and platforms were used in different stages to obtain the LST thermal surface behavior and to identify the LCZ classes. Their frequency and information, such as the operator and temporal and spatial resolution, are shown in Table 3 and Figure 6.

Table 3. Information about satellites and sensors used in the reviewed articles.

Preprints (www.preprints.org) | NOT PEER-REVIEWED | Posted: 15 December 2022 doi:10.20944/preprints202212.0260.v1

Satellites	Sensors	Operators	Publications	Time Resolution	Spatial Resolution
Terra-Aqua	MODIS	NASA	18	1-2 days	250m-1km
Terra	ASTER	NASA	8	16 days	15-90m
Landsat 8	OLI/TIRS	NASA/USGS	43	16 days	OLI: 15/30m TIRS: 100m
Landsat 7	ETM+	NASA/USGS	6	16 days	15-30-60m
Landsat 5	TM	NASA/USGS	6	16 days	30-120m
Sentinel 2 A-B	MSI	ESA	7	5 days	10m
FY-2F	--	NSMC	2	--	--
Others	--	--	9	--	--

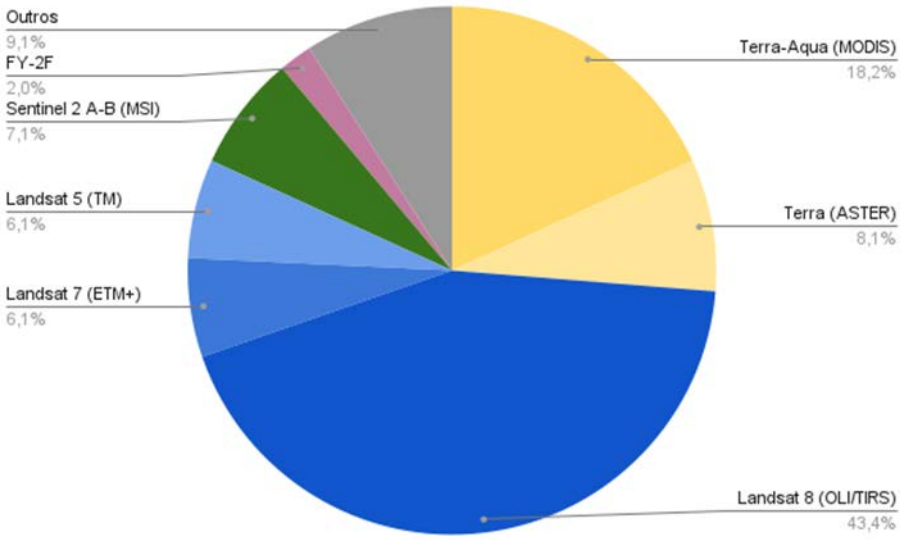

Figure 6. Satellites and sensors by publication.

The Landsat series is managed by the National Aeronautics and Space Administration (NASA) and the US Geological Survey (USGS) and involved the launch to the moment of nine satellites, of which Landsat 5, 7, and 8 were used by the revised articles, covering 55% all the publications. The satellite of the series most used in the reviewed articles was Landsat 8, which was launched in 2013, and operates with the Operational Land Imager (OLI) instruments and the Thermal Infrared Sensor (TIRS). The OLI sensor has spectral bands that collect data in the visible range, near-infrared and infrared of short waves, and a panchromatic band, with spatial resolution from 15 to 30 meters and 16 days of temporal resolution. The thermal sensor has two bands, with 100 meters spatial resolution [18].

In addition to the Landsat satellites, the AQUA and TERRA satellites are part of the Earth Observation System (EOS), a program founded by NASA and developed in partnership with Japan and Brazil, launched in 2002. The TERRA satellite was launched in 1999, involving aerospace agencies from Canada and Japan. The MODIS sensor is on board these two satellites, which can acquire Earth images from 1 to 2 days, with a spatial resolution of 250, 500, and 1000 meters. This sensor was used in approximately 18% of all revised articles. In addition, the TERRA satellite has in its instruments the ASTER sensor, which offers better spatial resolution, reaching 15 meters for the visible and near-infrared region, 30 meters for the short wave infrared region, and 90 meters for the thermal bands [19-21].

In general, Landsat and TERRA/AQUA sensors were more often used due to the long historical series and the free acquisition cost. However, although Landsat 8 provides the thermal data at a good spatial resolution of 100 meters, their 16 days revisit time is too

Preprints (www.preprints.org) | NOT PEER-REVIEWED | Posted: 15 December 2022 doi:10.20944/preprints202212.0260.v1

long. However, with Landsat 7, 8, and 9 in operation, this temporal resolution could decrease to five days. In contrast, the MODIS sensor provides its data in a shorter revisit period, although the thermal data spatial resolution is rougher, with 1 km. Therefore, one of the remote sensing challenges is acquiring surface temperature data in high spatial and temporal resolution, which is currently not possible [22].

The satellites and sensors highlighted as "others" are those that had only one occurrence in the reviewed articles, such as Worldview 3 used in [23], Meteosat Seviri in [23], Sentinel 1 A-B Multispectral Instrument (MSI) operated by [25], PROBA-V: Copernicus Global Land Cover Layers (CGLS-LC) 100 in [26], ECOSTRESS used in [27], Copernicus Global Cover maps (C-GLOPS) also in [27], NECP-GR data by [28], Gaofen-1 in [29] and Visible Infrared Imaging Radiometer Suite (VIIRS) by [30].

In addition to satellite images, one alternative is non-orbital data use, such as obtained by unmanned aerial vehicles (UAV) and aerodynamic twin engines. Their main advantage is the high spatial and temporal resolution, which is very useful for obtaining land surface temperature and their analysis in specific local climate zones. However, the operational cost of these tools is still relatively high [31].

3.4. Method to Obtain the Land Surface Temperature (LST)

Land Surface Temperature (LST) is essential for surface urban heat island studies. Usually, it is not measured directly by remote sensors, requiring mathematical methods to be estimated. Therefore, the methods used in the LST calculations used by the articles reviewed were cataloged and presented in Figure 7.

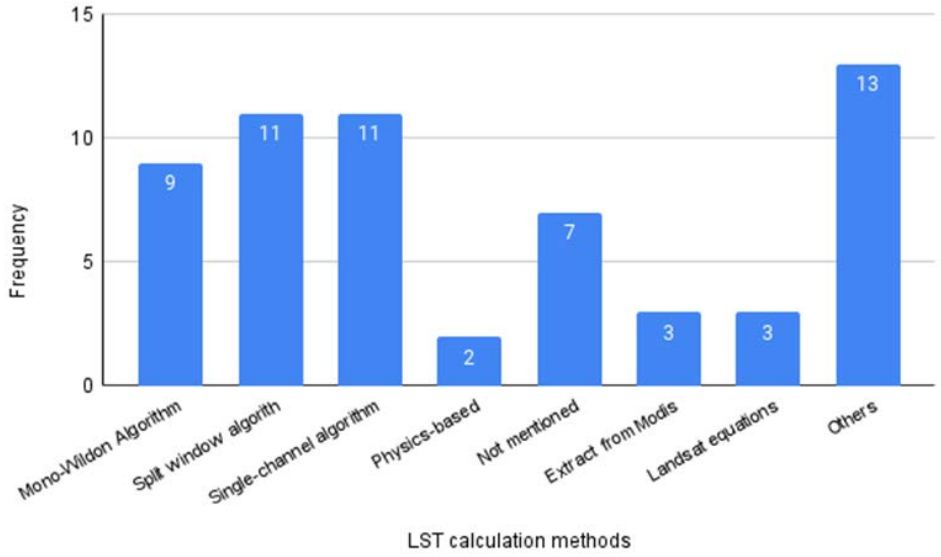

Figure 7. Land Surface Temperature (LST) calculation Methods.

Many LST estimation algorithms have been proposed and can be classified, according to [32], into three categories: Single-channel algorithms (SCA), Multi-channel, and Split-Window Algorithms (SWA). Together they account for 52% of the methods used in the articles reviewed to obtain LST.

The SCA advantage is that it estimates the LST with only one thermal channel. Thus, this method is the only one that can be applied to the Landsat platform with a thermal channel, such as the Landsat 4, 5, and 7 TM bands [33]. However, according to [34], the SWA is the best for calculating the LST from satellite data to understand SUHI. This method requires simultaneous data from at least two sensor channels, requiring only the atmospheric moisture content and surface emissivity as the parameters. The Statistical Mono-Window Algorithm (MWA) uses the thermal band brightness temperature, mean,

Preprints (www.preprints.org) | NOT PEER-REVIEWED | Posted: 15 December 2022 doi:10.20944/preprints202212.0260.v1

and surface emissivity difference to estimate the LST [35]. The equations of the three algorithms mentioned can be seen in Table 04.

Table 4. Equations of LST estimation algorithms.

Index	Equations	Authors
Split-Window Algorithm (SWA)	$Ts = C + (A1 + A2 (1-e/e) + A3 (\Delta e/e^2)) T4+T5/2 + (B1 + B2 (1-e/e) + B3(\Delta e/e^2) T4-T5/2$	[36]
Single-channel Algorithm (SCA)	$Ts = y1e(\psi 1 Lsen + \psi 2) + \psi 3 + \delta$	[33]
Mono-Window Algorithm (MWA)	$LST = B(LST)/(\ln e(\lambda.B(LST)/p+1))$	[37]

The LST calculation methods obtained through algorithms already implemented in software such as ENVI-met, Google Earth Engine, ArcGIS, and QGIS classification plugin were also widespread in the revised articles. Using friendlier software to obtain LST has become increasingly common and generally increases the number of users. In addition, it is worth highlighting they were used not only to get the LST but also to calculate the SUHI and the LCZ, among others.

It is notorious that the method classified as "others" is the most often found in our review, reaching 13 in this category. Still, it is worth noting that among them, some are used only once, such as the Two-channel algorithm [30], Algorithm Practical Single-channel [28], and Normalized Emissivity Method (NEM) [16]. Furthermore, 12% of the studies do not inform the method to classify the LST, which is a problem for replicating the methodology.

3.5. Surface Urban Heat Island (SUHI) Calculation

The surface urban heat islands (SUHI) are commonly calculated as the difference between the LST in urban and rural areas, according to [31], as illustrated in Figure 8. However, there are several proposals for calculating SUHI because not every urban cluster will be the same, and the urban and rural border areas are sometimes difficult to discriminate [30].

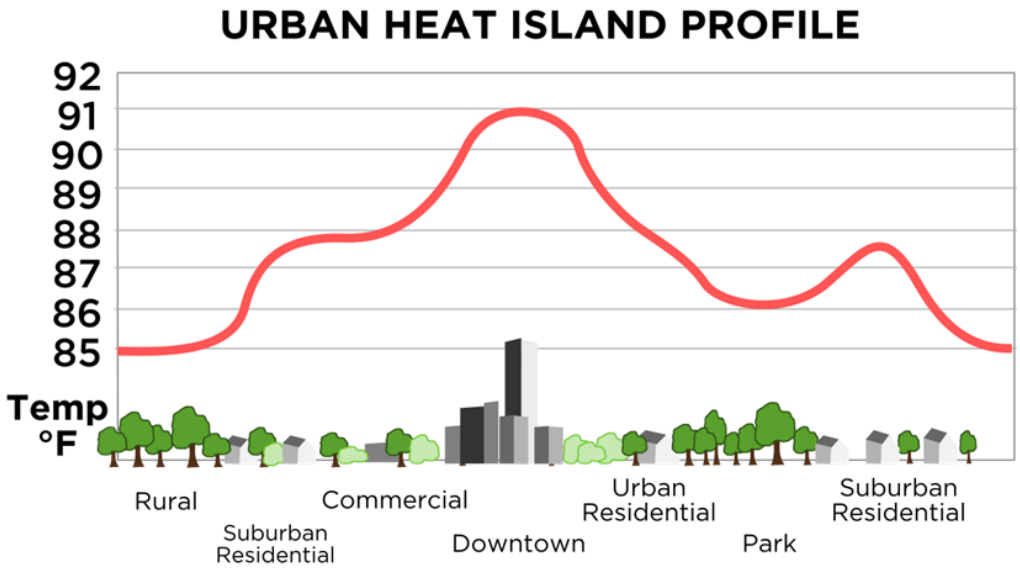

Figure 8. Urban Heat Island representation. Source [9].

 doi:10.20944/preprints202212.0260.v1

Therefore, all SUHI calculation methods found in the articles reviewed were cataloged and shown in Figure 9.

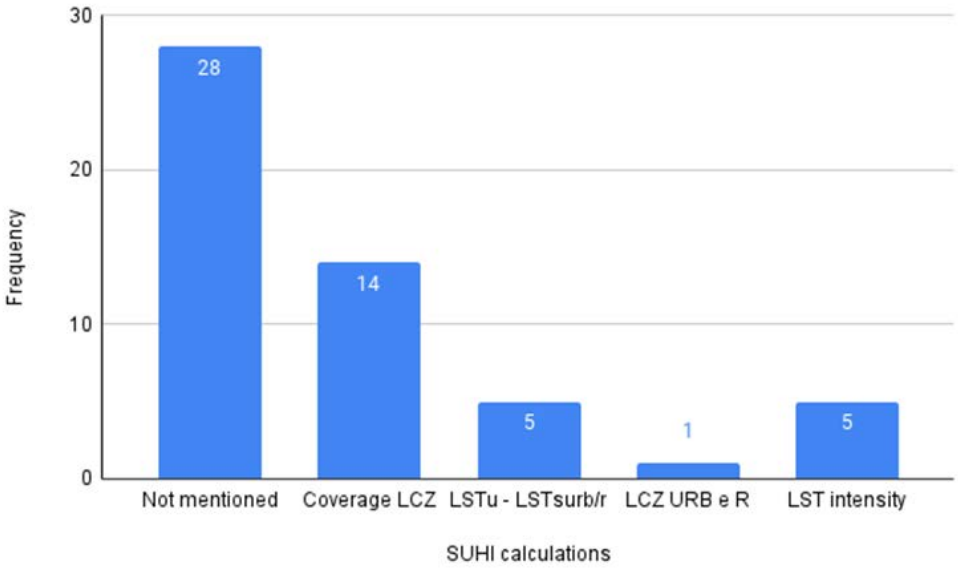

Figure 9. SUHI calculation methods. LSTu is the LST of the urban area; LSTsurb/r is the LST of the suburban and rural areas.

In more than half of the articles reviewed, the SUHI calculation method was not mentioned. This is a problem since it is essential in the article's methodology to present all the steps to get to the results. One explanation is that not all research focuses on identifying the heat islands, only verifying the LST effects on each LULC class.

From the articles in which the SUHI method was mentioned, the majority, about 56%, used the difference between the LST average of LCZ built and land cover types. This last one is usually class D, representing low vegetation such as grasslands or herbaceous plants/crops (see Figure 1). In addition, only [38] used another LCZ land cover class as a reference, which used class B, which means scattered trees with mostly pervious land. However, only using LCZ classes to improve the SUHI calculation is considered an improvement in the research's articles [5,39].

Other methods used to differentiate SUHI in urban and suburban/rural areas appear in 20% of the articles reviewed. While [35,40] uses the traditional SUHI method, consisting of the difference between the urban and rural areas LST, other studies, such as [41,42], only analyze the study area using the LST intensity and heat maps.

3.6. Method To Obtain The Local Climate Zones

Some methods are used in the literature to obtain the local climate zones (LCZ). The most used among the articles reviewed is shown in Figure 10.

Preprints (www.preprints.org) | NOT PEER-REVIEWED | Posted: 15 December 2022 doi:10.20944/preprints202212.0260.v1

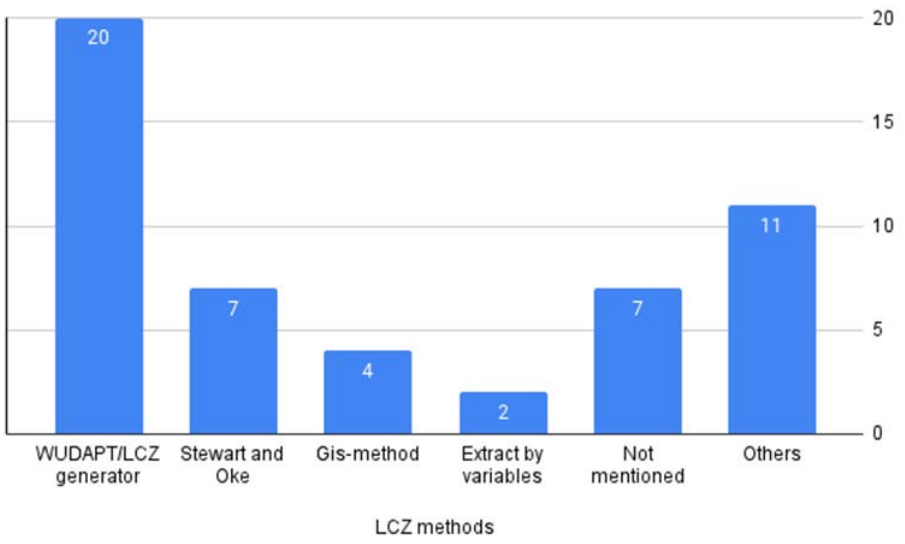

Figure 10. Methods of LCZ calculation.

The method that appears the most, with 39% among all publications, is from the World Urban Database and Access Portal Tools (WUDAPT). According to [5], it provides instructions for the LCZ classification using open access data and software, and the classification system consists basically of 1) data processing: including satellite image obtention, usually using Landsat; 2) selection of training and verification samples using a visual interpretation method with Google Earth images; 3) LCZ classification: Based on the samples obtained previously using the Random Forest classifier in some Geographic Information System (GIS) software, such as the System for Automated Geoscientific Analyses (SAGA), and finally the; 4) Accuracy assessment: using confusion matrix, the Kappa coefficient, and general precisions. After these steps, if the LCZ classification is not considered good, the training and verification samples should be collected again until a good map accuracy is reached.

The "others" LCZ classification methods appear in 21%, corresponding to unique ways with an appearance in only one article each. It generally used approaches already adopted in software, such as the QGIS plugin, as the [13] study, the Copernicus LCZ generating tool seen in [43] research, and methods based on previous studies such as those of [44,45].

In about 13% of the articles reviewed, Stewart and Oke's methodology was used, such as the [46,47] articles. This LCZ classification method consists of 1) Local data collections: where it is proposed to visit the site for data collection such as building geometries, land cover, and population density, among others. It is recommended to use secondary sources such as aerial photographs, satellite images, or land use and cover maps only if it is not possible to visit the studied area; 2) Set the thermal source: which are usually weather stations but can be adapted for optical sensors; and finally the 3) Selection of local climate zones: based in the data of step 1. In addition, the authors also raised the possibility of adapting the LCZ classes by joining two or more of them or even creating new ones, such as the snow cover for cold places [6]. It is also important to highlight that in approximately 13% of the articles, the LCZ methodology was not mentioned.

3.7. Variables Associated With SUHI and LCZ

Some variables associated with SUHI identification used in conjunction with LCZs were cataloged in this systematic review and shown in Figure 11. Of these variables, three of them were based on spectral indices presented in Table 5.

Preprints (www.preprints.org) | NOT PEER-REVIEWED | Posted: 15 December 2022 doi:10.20944/preprints202212.0260.v1

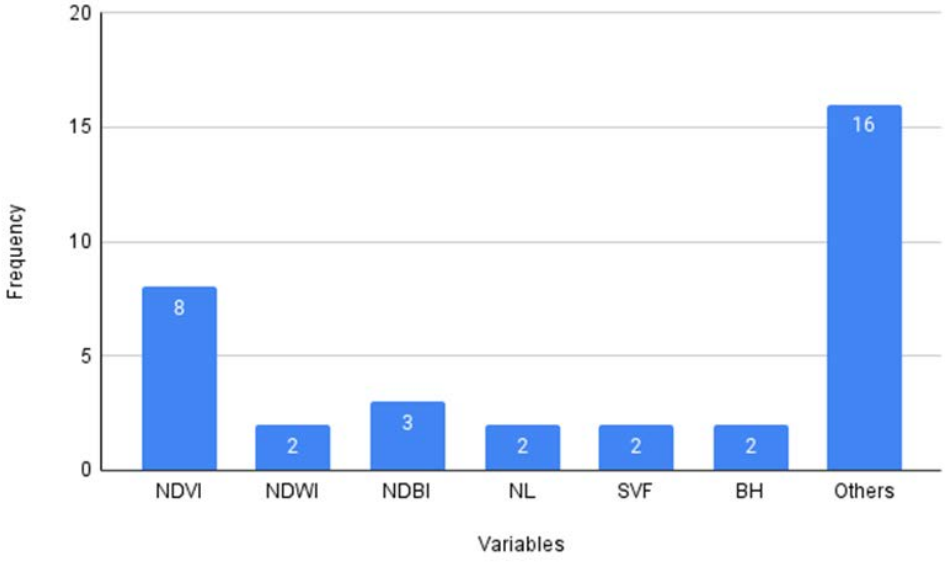

Figure 11. Variables associated with SUHI and LCZ used in the articles reviewed.

Table 5. Equations of principal spectral indexes used in the articles reviewed.

Index	Equations	Authors
Normalized Difference Vegetation Index (NDVI)	NDVI = (NIR – R)/(NIR + R)	[48]
Normalized Difference Water Index (NDWI)	NDWI = (NIR – SWIR)/(NIR + SWIR)	[49]
Normalized Difference Building (NDBI)	NDBI = (SWIR – NIR)/(SWIR + NIR)	[50]

The NDVI is one of the most well-known and used spectral indexes in the articles reviewed, with 23%. It was proposed by [48], and it is obtained by a normalized equation of reflectance in the NIR (near infrared) and R (Red) bands, with values ranging from -1 to +1. This index was used in studies such as [40], where the index allows for analyzing the vegetation spatial distribution difference in urban and rural areas.

Other spectral indices mostly used were the Normalized Difference Water Index (NDWI) and Normalized Difference Building (NDBI), which appeared in 14% of the studies. For example, [43] also used them with the NDVI as conditional arguments for pixel size reclassification and LST variables for the prediction model.

The category cited as "others" among the variables associated with SUHI and LCZ was the most frequent, with 46%. However, all the variables are only used once considered in all the articles reviewed. Some are related to population, such as in [50], used to determine the urban thermal environment influence. Another one is the heat island ratio, an index generated by [51] that makes temperatures of different years comparable. Further, Night Lights (NL), Sky View Factor (SVF), and Building Height (BH) appeared in 5,7% of studies, respectively.

In addition, although it is not a variable, many studies used statistical methods to improve their analysis and results among the articles reviewed and were also cataloged in this systematic review and presented in Figure 12.

Preprints (www.preprints.org) | NOT PEER-REVIEWED | Posted: 15 December 2022 doi:10.20944/preprints202212.0260.v1

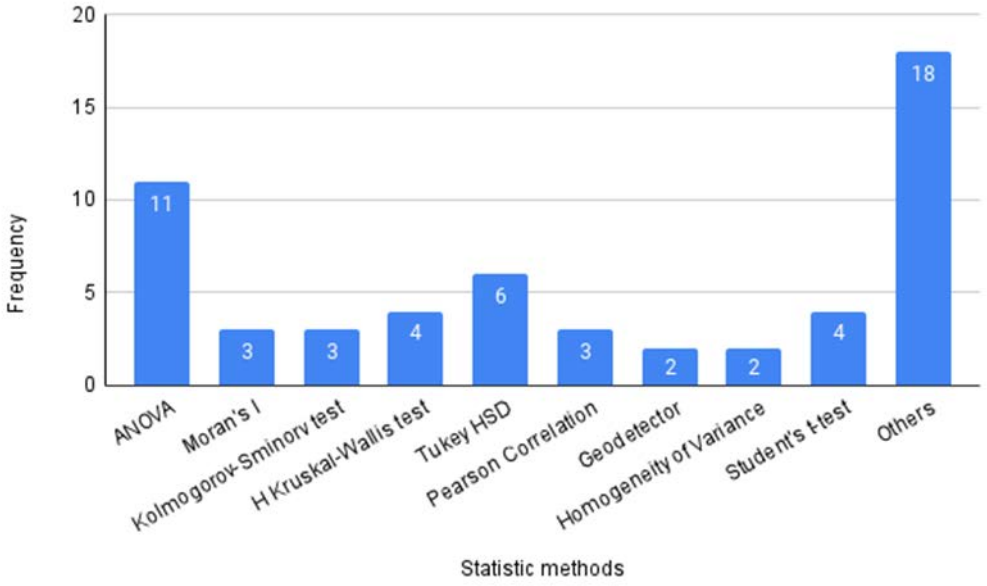

Figure 12. Statistic methods used by the articles reviewed.

The analysis of variance (ANOVA) was the most statistical method found in 20% of studies. Generally, it is used to decide whether the observed sample differences are real, caused by significant differences in the populations or if they are casual, resulting from the sample variability. Thus, this analysis goes from the assumption that chaos produces slight deviations while significant differences are generated by natural causes [52]. In the articles reviewed, the ANOVA was used to examine the significance of the difference among the thermal groups.

Together with ANOVA, the Tukey test, also known as Tukey Honestly Significance Difference (HSD), was found in 11% of studies. It was used to determine which pair of LCZ is significantly different in terms of LST mean. Studies using these two statistical methods were those of [53-55].

In addition to these methods, many others are used, as highlighted in the "Others" category, demonstrating the statistical procedure's importance for better evaluating the LST and LCZ correlations.

3.8. Most Used Software

In the SUHI and LCZ studies, using more than one software is expected. In this systematic review, the most used software in the articles reviewed was cataloged and shown in Figure 13.

Preprints (www.preprints.org) | NOT PEER-REVIEWED | Posted: 15 December 2022 doi:10.20944/preprints202212.0260.v1

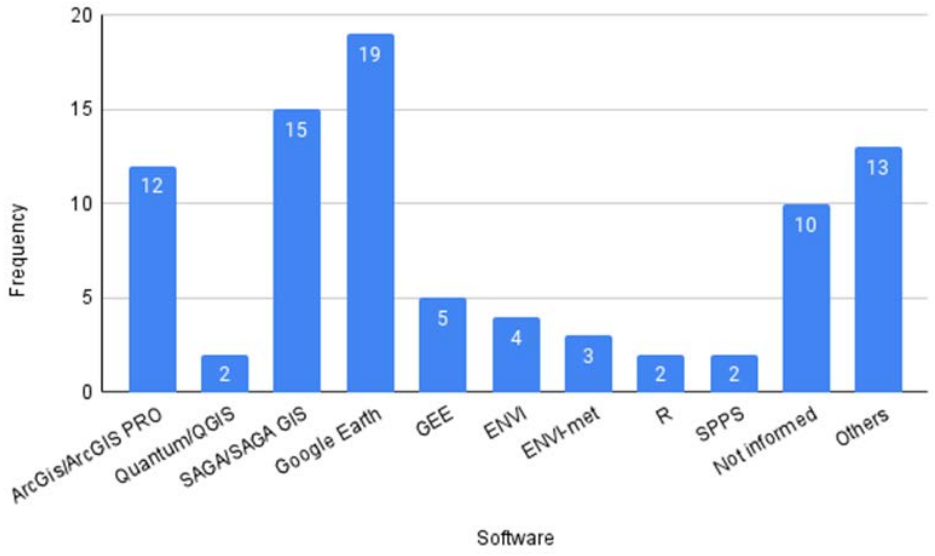

Figure 13. Software most used in the reviewed articles. GEE is Google Earth Engine; ENVI is Environment for Visualizing Images; R is R language; SPPS is Statistics Package for the Social Science.

Google Earth is the most widely used software in 22% of the studies, followed by SAGA/GIS in 17%. The first is a program developed by Google, providing a three-dimensional model of the globe built from satellite image mosaics. Thus, using this software, it is possible to identify features, places, constructions, cities, and landscapes. More information about it is available at (https://www.google.com.br/intl/pt-BR/earth/). While SAGA/GIS, a free GIS software, is used as an effective spatial algorithms implementation providing a set of geostatistical methods. More information about it is available at the link (https://saga-gis.sourceforge.io/en/index.html). This two software were widely used to generate the LCZ maps, Google Earth for collecting training and verification samples, and the SAGA/GIS to run the classifier, usually Random Forest, as mentioned in sub-section 3.6.

Another widely used software is ArcGIS, with a 14% appearance. During the reviews of the articles, it was observed that it was used for various functions, both for statistical analysis [53]; LST calculation [51], among others. Esri, a private company in geographic information services, maintains this platform. More information about it can be found at (https://www.esri.com/en-us/arcgis/products/arcgis-online/overview). A well-known software that replaces ArcGIS is QGIS. Its main advantage is that it is free-to-use software, although, in the systematic review, it had only been presented in a few studies.

4. Final Considerations

This systematic review evaluates the state of the art related to the use of local climatic zones to identify the surface urban heat islands through remote sensing techniques. It was revealed that the theme interest is very recent, has increased over the years, and has a growth trend in the future. Therefore, using the PRISMA method, it was identified 10,406 articles in the literature, which, after being submitted to the selection, eligibility, and, finally, inclusion steps, resulted in 51 articles. They were further analyzed, cataloged, presented, and discussed in this article using tables, cluster analysis figures, and maps.

Our main results demonstrate that among the satellite found in the publications, Landsat and TERRA/AQUA sensors appeared the most, with 82%. However, there is a tendency for other sensors to be used, such as Sentinel 2, with 7% appearances. Regarding the methods to obtain LST, the Split Window and Single-Channel Algorithm were the most used, reaching more than 26% each. For the SUHI calculation, more than half of the

 doi:10.20944/preprints202212.0260.v1

articles did not inform or detail the methodology used. However, in 56% of the articles, the difference between the LST average of a given LCZ urban and land cover class was used, demonstrating the concern of scholars to improve the SUHI calculation considering the LCZ. For the LCZ classification, the WUDAPT method is still the one that appears the most, occurring in 39% of publications. In addition, three spectral indices, NDVI, NDWI, and NDBI, were the most found among all the variables related to SUHI and LCZ. However, several other variables appeared, some of them just once. It is worth pointing out that many statistical methods were used for better analysis of LST and LCZ, demonstrating the importance of these methods for assessing the correlations among them and highlighting ANOVA as the most used statistical method. For last, the most used software was Google Earth and SAGA/GIS, widely used to obtain the LCZ maps, justifying the frequency of their appearances.

It is worth noting that this study has some limitations, such as the article's method choice, which used the Scopus database. However, to mitigate this problem some other articles from other databases were included in this systematic review. Finally, considering the current climatic changes, this systematic review is a reference for news studies on surface urban heat island identification through local climate zones in different areas of the world using remote sensing data to estimate the land surface temperature. Consequently, these studies can help decision-makers to mitigate these effects.

Author Contributions: "Conceptualization and Methodology, R.F. and VN.; software, R.F.; Formal Analysis and Investigation, V.N., M.F., R.F., J.O.; data curation and writing—original draft preparation, R.F.; writing—review and editing, V.N.; supervision, V.N., M.F.; funding acquisition, J.O. All authors have read and agreed to the published version of the manuscript."

Funding: The R.F. was funded by a scholarship from Coordenação de Aperfeiçoamento de Pessoal Nível Superior from Brazil.

Acknowledgments: The authors thank the National Institute for Space Research (INPE), Rio Grande do Sul Federal University (UFRGS), and the Federal University of ABC (UFABC) for the support given during this research

Conflicts of Interest: The authors declare no conflict of interest.

 doi:10.20944/preprints202212.0260.v1

Appendix A

Table A1. Articles read in the systematic review.

Title	Year of publication	Authors
Dynamics and controls of urban heat sink and island phenomena in a desert city: Development of a local climate zone scheme using remotely-sensed inputs	2016	[22]
Analysis of land use change and expansion of surface urban heat island in Bogor city by remote sensing	2018	[53]
Understanding Land Surface Temperature Differences of Local Climate Zones Based on Airborne Remote Sensing Data	2018	[16]
Analysis of the Spatial and Temporal Variations of Land Surface Temperature Based on Local Climate Zones: A Case Study in Nanjing, China	2019	[29]
Detecting multi-temporal land cover change and land surface temperature in Pearl River Delta by adopting local climate zone	2019	[15]
Enhanced geographic information system-based mapping of local climate zones in Beijing, China	2019	[56]
Impact of atmospheric conditions and levels of urbanization on the relationship between nocturnal surface and urban canopy heat islands	2019	[47]
Inter-/intra-zonal seasonal variability of the surface urban heat island based on local climate zones in three central European cities	2019	[57]
Multi-Temporal Effects of Urban Forms and Functions on Urban Heat Islands Based on Local Climate Zone Classification	2019	[46]
Seasonality of Surface Urban Heat Island in Delhi City Region Measured by Local Climate Zones and Conventional Indicators	2019	[54]
SUHI analysis using Local Climate Zones—A comparison of 50 cities	2019	[58]
Urban design factors influencing surface urban heat island in the high-density city of Guangzhou based on the local climate zone	2019	[44]
Annual and monthly analysis of surface urban heat island intensity with respect to the local climate zones in Budapest	2020	[59]
Evaluation of urban heat islands using local climate zones and the influence of sea-land breeze.	2020	[14]
Inter-local climate zone differentiation of land surface temperatures for Management of Urban Heat in Nairobi City, Kenya	2020	[60]
Mapping Local Climate Zones Using ArcGIS-Based Method and	2020	[61]

 doi:10.20944/preprints202212.0260.v1

Exploring Land Surface Temperature Characteristics in Chenzhou, China		
Optimizing local climate zones to mitigate urban heat island effect in human settlements	2020	[4]
Remote sensing of urban thermal environments within local climate zones: A case study of two high-density subtropical Chinese cities	2020	[62]
Spatial and temporal analysis of the increasing effects of large-scale infrastructure construction on the surface urban heat island	2020	[51]
Spatiotemporal Changes in the Urban Heat Island Intensity of Distinct Local Climate Zones: Case Study of Zhongshan District, Dalian, China	2020	[38]
The local climate impact of an African city during clear-sky conditions—Implications of the recent urbanization in Kampala (Uganda)	2020	[24]
Urban Spatial Patterns and Heat Exposure in the Mediterranean City of Tel Aviv	2020	[47]
Use of Local Climate Zones to investigate surface urban heat islands in Texas	2020	[63]
Using local climate zones to compare remotely sensed surface temperatures in temperate cities and hot desert cities	2020	[40]
A cooled city? Comparing human activity changes on the impact of urban thermal environment before and after city-wide lockdown	2021	[50]
A practical approach of urban green infrastructure planning to mitigate urban overheating: A case study of Guangzhou	2021	[42]
An application of the LCZ approach in surface urban heat island mapping in Sofia, Bulgaria	2021	[31]
Analyses of land surface temperature (LST) variability among local climate zones (LCZs) comparing Landsat-8 and ENVI-met model data	2021	[13]
Combination of Sentinel-2 and PALSAR-2 for Local Climate Zone Classification: A Case Study of Nanchang, China	2021	[25]
Dynamic changes of local climate zones in the Guangdong-hong kong-Macao greater bay area and their spatial-temporal impacts on the surface urban heat island effect between 2005 and 2015	2021	[64]
Evaluation of seasonal variability in magnitude of urban heat islands using local climate zone classification and surface albedo	2021	[41]
Exploring diurnal thermal variations in urban local climate zones with	2021	[27]

 doi:10.20944/preprints202212.0260.v1

ECOSTRESS land surface temperature data		
Exploring the relationship between urban form and land surface temperature (LST) in a semi-arid region case study of Ben Guerir city - Morocco	2021	[35]
LCZ scheme for assessing Urban Heat Island intensity in a complex urban area (Beirut, Lebanon)	2021	[65]
Local climate zones and thermal characteristics in Riyadh City, Saudi Arabia	2021	[66]
Local climate zones mapping using object-based image analysis and validation of its effectiveness through urban surface temperature analysis in China	2021	[28]
Seasonal SUHI analysis using local climate zone classification: A case study of Wuhan, china	2021	[67]
Spatial variability and temporal heterogeneity of surface urban heat island patterns and the suitability of local climate zones for land surface temperature characterization	2021	[12]
Spatiotemporal characteristics of the surface urban heat island and its driving factors based on local climate zones and population in Beijing, china	2021	[5]
The suitability of the urban local climate zone classification scheme for surface temperature studies in distinct macroclimate regions	2021	[68]
Time Evolution of the Surface Urban Heat Island	2021	[69]
Urban Thermal Characteristics of Local Climate Zones and Their Mitigation Measures across Cities in Different Climate Zones of China	2021	[55]
An urban energy balance-guided machine learning approach for synthetic nocturnal surface Urban Heat Island prediction: A heatwave event in Naples	2022	[43]
Analysis of surface urban heat islands based on local climate zones via spatiotemporally enhanced land surface temperature	2022	[30]
Diurnally continuous dynamics of surface urban heat island intensities of local climate zones with spatiotemporally enhanced satellite-derived land surface temperatures	2022	[39]
Estimation of the Urban Heat Island Effect in a Reformed Urban District: A Scenario-Based Study in Hong Kong	2022	[70]
Geographical Detection of Urban Thermal Environment Based on the Local Climate Zones: A Case Study in Wuhan, China	2022	[71]
Identification of SUHI in Urban Areas by Remote Sensing Data and	2022	[23]

 doi:10.20944/preprints202212.0260.v1

Mitigation Hypothesis through Solar Reflective Materials		
Spatiotemporal evolution of urban development and surface urban heat island in Guangdong-Hong Kong-Macau greater bay area of China from 2013 to 2019	2022	[72]
The role of blue green infrastructure in the urban thermal environment across seasons and local climate zones in East Africa	2022	[26]
Using Local Climate Zones to investigate Spatio-temporal evolution of thermal environment at the urban regional level: A case study in Xi'an, China	2022	[32]

References

1. United Nations. Available online: https://www.un.org/development/desa/en/news/population/2018-revision-of-world-urbanization-prospects.html (accessed on 09 August 2022).
2. Dewan, A.; Kiselev, G.; Botje, D. Diurnal and Seasonal Trends and Associated Determinants of Surface Urban Heat Islands in Large Bangladesh Cities. *Applied Geography* **2021**, *135*, 102533. https://doi.org/10.1016/j.apgeog.2021.102533.
3. Sobrino J.A; Irakulis I. A. Methodology for Comparing the Surface Urban Heat Island in Selected Urban Agglomerations Around the World from Sentinel-3 SLSTR Data. *Remote Sens*. 2020, 12, 2052.
4. Yang, J.; Wang, Y.; Xiu, C.; Xiao, X.; Xia, J.; Jin, C. Optimizing Local Climate Zones to Mitigate Urban Heat Island Effect in Human Settlements. *Journal of Cleaner Production* **2020**, *275*, 123767. https://doi.org/10.1016/j.jclepro.2020.123767.
5. Zhang, Y.; Li, D.; Liu, L.; Liang, Z.; Shen, J.; Wei, F.; Li, S. Spatiotemporal Characteristics of the Surface Urban Heat Island and Its Driving Factors Based on Local Climate Zones and Population in Beijing, China. *Atmosphere* **2021**, *12* (10), 1271. https://doi.org/10.3390/atmos12101271.
6. Stewart, I. D.; Oke, T. R. Local Climate Zones for Urban Temperature Studies. *Bulletin of the American Meteorological Society* **2012**, *93* (12), 1879–1900. https://doi.org/10.1175/BAMS-D-11-00019.1.
7. Demuzere, M.; Kittner, J.; Bechtel, B. LCZ Generator: A Web Application to Create Local Climate Zone Maps. *Front. Environ. Sci.* **2021**, *9*, 637455. https://doi.org/10.3389/fenvs.2021.637455.
8. Souza, C. A. de; Paranhos Filho, A. C.; Guaraldo, E. IDENTIFICAÇÃO E CARACTERIZAÇÃO DA PAISAGEM URBANA E ENTORNO RURAL DE CAMPO GRANDE. *R. gest. sust. ambient.* **2020**, *9* (0I), 263. https://doi.org/10.19177/rgsa.v9e0I2020263-286.
9. Lehnert, M.; Savić, S.; Milošević, D.; Dunjić, J.; Geletič, J. Mapping Local Climate Zones and Their Applications in European Urban Environments: A Systematic Literature Review and Future Development Trends. *IJGI* **2021**, *10* (4), 260. https://doi.org/10.3390/ijgi10040260.
10. Xue, J.; You, R.; Liu, W.; Chen, C.; Lai, D. Applications of Local Climate Zone Classification Scheme to Improve Urban Sustainability: A Bibliometric Review. *Sustainability* **2020**, *12* (19), 8083. https://doi.org/10.3390/su12198083.
11. Viana, J.; Santos, J.; Neiva, R.; Souza, J.; Duarte, L.; Teodoro, A.; Freitas, A. Remote Sensing in Human Health: A 10-Year Bibliometric Analysis. *Remote Sensing* **2017**, *9* (12), 1225. https://doi.org/10.3390/rs9121225.
12. Zhao, Z.; Sharifi, A.; Dong, X.; Shen, L.; He, B.-J. Spatial Variability and Temporal Heterogeneity of Surface Urban Heat Island Patterns and the Suitability of Local Climate Zones for Land Surface Temperature Characterization. *Remote Sensing* **2021**, *13* (21), 4338. https://doi.org/10.3390/rs13214338.
13. Unal Cilek, M.; Cilek, A. Analyses of Land Surface Temperature (LST) Variability among Local Climate Zones (LCZs) Comparing Landsat-8 and ENVI-Met Model Data. *Sustainable Cities and Society* **2021**, *69*, 102877. https://doi.org/10.1016/j.scs.2021.102877.
14. Zhou, X.; Okaze, T.; Ren, C.; Cai, M.; Ishida, Y.; Watanabe, H.; Mochida, A. Evaluation of Urban Heat Islands Using Local Climate Zones and the Influence of Sea-Land Breeze. *Sustainable Cities and Society* **2020**, *55*, 102060. https://doi.org/10.1016/j.scs.2020.102060.
15. Wang, R.; Cai, M.; Ren, C.; Bechtel, B.; Xu, Y.; Ng, E. Detecting Multi-Temporal Land Cover Change and Land Surface Temperature in Pearl River Delta by Adopting Local Climate Zone. *Urban Climate* **2019**, *28*, 100455. https://doi.org/10.1016/j.uclim.2019.100455.
16. Bartesaghi Koc, C.; Osmond, P.; Peters, A.; Irger, M. Understanding Land Surface Temperature Differences of Local Climate Zones Based on Airborne Remote Sensing Data. *IEEE J. Sel. Top. Appl. Earth Observations Remote Sensing* **2018**, *11* (8), 2724–2730. https://doi.org/10.1109/JSTARS.2018.2815004.
17. van Eck, N. J.; Waltman, L. VOSviewer Manual. 53.

18. USGS. Available online: https://www.usgs.gov/landsat-missions/landsat-satellite-missions (accessed on 28 June 2022).
19. NASA. Available online: http://aqua.nasa.gov/ (accessed on 28 June 2022).
20. NASA. Available online: http://www.nasa.gov/mission_pages/terra/index.html (accessed on 28 June 2022).
21. SATTELITE IMAGING CORPORATION. Available online: www.satimagingcorp.com/satellite-sensors/aster.html (acessed on 28 June 2022).
22. Nassar, A. K.; Blackburn, G. A.; Whyatt, J. D. Dynamics and Controls of Urban Heat Sink and Island Phenomena in a Desert City: Development of a Local Climate Zone Scheme Using Remotely-Sensed Inputs. *International Journal of Applied Earth Observation and Geoinformation* **2016**, *51*, 76–90. https://doi.org/10.1016/j.jag.2016.05.004.
23. Costanzini, S.; Despini, F.; Beltrami, L.; Fabbi, S.; Muscio, A.; Teggi, S. Identification of SUHI in Urban Areas by Remote Sensing Data and Mitigation Hypothesis through Solar Reflective Materials. *Atmosphere* **2021**, *13* (1), 70. https://doi.org/10.3390/atmos13010070.
24. BROUSSE, O.; WOUTERS, H.; DEMUZERE, M.; THIERY, W.; WALLE, J. V.; LIPZIG, N. P. M. The Local Climate Impact of an African City During Clear-Sky Conditions-Implications of the Recent Urbanization in Kampala (Uganda). *International Journal of Climatology* **2020**, *40*, *4586-4608*. https://doi.org/10.1002/joc.6477.
25. Chen, C.; Bagan, H.; Xie, X.; La, Y.; Yamagata, Y. Combination of Sentinel-2 and PALSAR-2 for Local Climate Zone Classification: A Case Study of Nanchang, China. *Remote Sensing* **2021**, *13* (10), 1902. https://doi.org/10.3390/rs13101902.
26. Li, X.; Stringer, L. C.; Dallimer, M. The Role of Blue Green Infrastructure in the Urban Thermal Environment across Seasons and Local Climate Zones in East Africa. *Sustainable Cities and Society* **2022**, *80*, 103798. https://doi.org/10.1016/j.scs.2022.103798.
27. Chang, Y.; Xiao, J.; Li, X.; Middel, A.; Zhang, Y.; Gu, Z.; Wu, Y.; He, S. Exploring Diurnal Thermal Variations in Urban Local Climate Zones with ECOSTRESS Land Surface Temperature Data. *Remote Sensing of Environment* **2021**, *263*, 112544. https://doi.org/10.1016/j.rse.2021.112544.
28. Ma, L.; Yang, Z.; Zhou, L.; Lu, H.; Yin, G. Local Climate Zones Mapping Using Object-Based Image Analysis and Validation of Its Effectiveness through Urban Surface Temperature Analysis in China. *Building and Environment* **2021**, *206*, 108348. https://doi.org/10.1016/j.buildenv.2021.108348.
29. Hu, J.; Yang, Y.; Pan, X.; Zhu, Q.; Zhan, W.; Wang, Y.; Ma, W.; Su, W. Analysis of the Spatial and Temporal Variations of Land Surface Temperature Based on Local Climate Zones: A Case Study in Nanjing, China. *IEEE J. Sel. Top. Appl. Earth Observations Remote Sensing* **2019**, *12* (11), 4213–4223. https://doi.org/10.1109/JSTARS.2019.2926502.
30. Xia, H.; Chen, Y.; Song, C.; Li, J.; Quan, J.; Zhou, G. Analysis of Surface Urban Heat Islands Based on Local Climate Zones via Spatiotemporally Enhanced Land Surface Temperature. *Remote Sensing of Environment* **2022**, *273*, 112972. https://doi.org/10.1016/j.rse.2022.112972.
31. Dimitrov, S.; Popov, A.; Iliev, M. An Application of the LCZ Approach in Surface Urban Heat Island Mapping in Sofia, Bulgaria. *Atmosphere* **2021**, *12* (11), 1370. https://doi.org/10.3390/atmos12111370.
32. Han, B.; Luo, Z.; Liu, Y.; Zhang, T.; Yang, L. Using Local Climate Zones to Investigate Spatio-Temporal Evolution of Thermal Environment at the Urban Regional Level: A Case Study in Xi'an, China. *Sustainable Cities and Society* **2022**, *76*, 103495. https://doi.org/10.1016/j.scs.2021.103495.
33. Jimenez-Munoz, J. C.; Cristobal, J.; Sobrino, J. A.; Soria, G.; Ninyerola, M.; Pons, X.; Pons, X. Revision of the Single-Channel Algorithm for Land Surface Temperature Retrieval From Landsat Thermal-Infrared Data. *IEEE Trans. Geosci. Remote Sensing* **2009**, *47* (1), 339–349. https://doi.org/10.1109/TGRS.2008.2007125.
34. Wang, M.; He, G.; Zhang, Z.; Wang, G.; Wang, Z.; Yin, R.; Cui, S.; Wu, Z.; Cao, X. A Radiance-Based Split-Window Algorithm for Land Surface Temperature Retrieval: Theory and Application to MODIS Data. *International Journal of Applied Earth Observation and Geoinformation* **2019**, *76*, 204–217. https://doi.org/10.1016/j.jag.2018.11.015.
35. Azmi, R.; Tekouabou Koumetio, C. S.; Diop, E. B.; Chenal, J. Exploring the Relationship between Urban Form and Land Surface Temperature (LST) in a Semi-Arid Region Case Study of Ben Guerir City - Morocco. *Environmental Challenges* **2021**, *5*, 100229. https://doi.org/10.1016/j.envc.2021.100229.
36. Zhengming Wan; Dozier, J. A Generalized Split-Window Algorithm for Retrieving Land-Surface Temperature from Space. *IEEE Trans. Geosci. Remote Sensing* **1996**, *34* (4), 892–905. https://doi.org/10.1109/36.508406.
37. Qin, Z.; Karnieli, A.; Berliner, P. A Mono-Window Algorithm for Retrieving Land Surface Temperature from Landsat TM Data and Its Application to the Israel-Egypt Border Region. *International Journal of Remote Sensing* **2001**, *22* (18), 3719–3746. https://doi.org/10.1080/01431160010006971.
38. Han, J.; Liu, J.; Liu, L.; Ye, Y. Spatiotemporal Changes in the Urban Heat Island Intensity of Distinct Local Climate Zones: Case Study of Zhongshan District, Dalian, China. *Complexity* **2020**, *2020*, 1–9. https://doi.org/10.1155/2020/8820338.
39. Dong, P.; Jiang, S.; Zhan, W.; Wang, C.; Miao, S.; Du, H.; Li, J.; Wang, S.; Jiang, L. Diurnally Continuous Dynamics of Surface Urban Heat Island Intensities of Local Climate Zones with Spatiotemporally Enhanced Satellite-Derived Land Surface Temperatures. *Building and Environment* **2022**, *218*, 109105. https://doi.org/10.1016/j.buildenv.2022.109105.
40. Fricke, C.; Pongrácz, R.; Gál, T.; Savić, S.; Unger, J. Using Local Climate Zones to Compare Remotely Sensed Surface Temperatures in Temperate Cities and Hot Desert Cities. *Moravian Geographical Reports* **2020**, *28* (1), 48–60. https://doi.org/10.2478/mgr-2020-0004.
41. Dutta, K.; Basu, D.; Agrawal, S. Evaluation of Seasonal Variability in Magnitude of Urban Heat Islands Using Local Climate Zone Classification and Surface Albedo. *Int. J. Environ. Sci. Technol.* **2021**. https://doi.org/10.1007/s13762-021-03602-w.

42. Wang, Y.; Ni, Z.; Hu, M.; Chen, S.; Xia, B. A Practical Approach of Urban Green Infrastructure Planning to Mitigate Urban Overheating: A Case Study of Guangzhou. *Journal of Cleaner Production* **2021**, *287*, 124995. https://doi.org/10.1016/j.jclepro.2020.124995.
43. Oliveira, A.; Lopes, A.; Niza, S.; Soares, A. An Urban Energy Balance-Guided Machine Learning Approach for Synthetic Nocturnal Surface Urban Heat Island Prediction: A Heatwave Event in Naples. *Science of The Total Environment* **2022**, *805*, 150130. https://doi.org/10.1016/j.scitotenv.2021.150130.
44. Shi, Y.; Xiang, Y.; Zhang, Y. Urban Design Factors Influencing Surface Urban Heat Island in the High-Density City of Guangzhou Based on the Local Climate Zone. *Sensors* **2019**, *19* (16), 3459. https://doi.org/10.3390/s19163459.
45. Feng, J.; Cai, X.; Chapman, L. Impact of Atmospheric Conditions and Levels of Urbanization on the Relationship between Nocturnal Surface and Urban Canopy Heat Islands. *Q.J.R. Meteorol. Soc.* **2019**, *145* (724), 3284–3299. https://doi.org/10.1002/qj.3619.
46. Quan, J. Multi-Temporal Effects of Urban Forms and Functions on Urban Heat Islands Based on Local Climate Zone Classification. *Int. J. Environ. Res. Public Health* **2019**, 35.
47. Mandelmilch, M.; Ferenz, M.; Mandelmilch, N.; Potchter, O. Urban Spatial Patterns and Heat Exposure in the Mediterranean City of Tel Aviv. *Atmosphere* **2020**, *11* (9), 963. https://doi.org/10.3390/atmos11090963.
48. Rouse, W.; Haas, R. H. MONITORING VEGETATION SYSTEMS IN THE GREAT PLAINS WITH ERTS. 9.
49. Gao, B. NDWI—A Normalized Difference Water Index for Remote Sensing of Vegetation Liquid Water from Space. *Remote Sensing of Environment* **1996**, *58* (3), 257–266. https://doi.org/10.1016/S0034-4257(96)00067-3.
50. Cai, Z.; Tang, Y.; Zhan, Q. A Cooled City? Comparing Human Activity Changes on the Impact of Urban Thermal Environment before and after City-Wide Lockdown. *Building and Environment* **2021**, *195*, 107729. https://doi.org/10.1016/j.buildenv.2021.107729.
51. Wan, J.; Yong, B.; Zhou, X. Spatial and Temporal Analysis of the Increasing Effects of Large-Scale Infrastructure Construction on the Surface Urban Heat Island. *Ecotoxicology and Environmental Safety* **2022**, *237*, 113521. https://doi.org/10.1016/j.ecoenv.2022.113521.
52. Martins, G. A.; Domingues, O. *Estatística Geral e aplicada*, 6rd ed.; Publisher: atlas, Brasil, 2017; pp. 1-360.
53. Nurwanda, A.; Honjo, T. Analysis of Land Use Change and Expansion of Surface Urban Heat Island in Bogor City by Remote Sensing. *IJGI* **2018**, *7* (5), 165. https://doi.org/10.3390/ijgi7050165.
54. Budhiraja, B.; Gawuc, L.; Agrawal, G. Seasonality of Surface Urban Heat Island in Delhi City Region Measured by Local Climate Zones and Conventional Indicators. *IEEE J. Sel. Top. Appl. Earth Observations Remote Sensing* **2019**, *12* (12), 5223–5232. https://doi.org/10.1109/JSTARS.2019.2955133.
55. Li, N.; Yang, J.; Qiao, Z.; Wang, Y.; Miao, S. Urban Thermal Characteristics of Local Climate Zones and Their Mitigation Measures across Cities in Different Climate Zones of China. *Remote Sensing* **2021**, *13* (8), 1468. https://doi.org/10.3390/rs13081468.
56. Quan, J. Enhanced Geographic Information System-Based Mapping of Local Climate Zones in Beijing, China. *Sci. China Technol. Sci.* **2019**, *62* (12), 2243–2260. https://doi.org/10.1007/s11431-018-9417-6.
57. Geletič, J.; Lehnert, M.; Savić, S.; Milošević, D. Inter-/Intra-Zonal Seasonal Variability of the Surface Urban Heat Island Based on Local Climate Zones in Three Central European Cities. *Building and Environment* **2019**, *156*, 21–32. https://doi.org/10.1016/j.buildenv.2019.04.011.
58. Bechtel, B.; Demuzere, M.; Mills, G.; Zhan, W.; Sismanidis, P.; Small, C.; Voogt, J. SUHI Analysis Using Local Climate Zones—A Comparison of 50 Cities. *Urban Climate* **2019**, *28*, 100451. https://doi.org/10.1016/j.uclim.2019.01.005.
59. Dian, C.; Pongrácz, R.; Dezső, Z.; Bartholy, J. Annual and Monthly Analysis of Surface Urban Heat Island Intensity with Respect to the Local Climate Zones in Budapest. *Urban Climate* **2020**, *31*, 100573. https://doi.org/10.1016/j.uclim.2019.100573.
60. Ochola, E. M.; Fakharizadehshirazi, E.; Adimo, A. O.; Mukundi, J. B.; Wesonga, J. M.; Sodoudi, S. Inter-Local Climate Zone Differentiation of Land Surface Temperatures for Management of Urban Heat in Nairobi City, Kenya. *Urban Climate* **2020**, *31*, 100540. https://doi.org/10.1016/j.uclim.2019.100540.
61. Chen, Y.; Zheng, B.; Hu, Y. Mapping Local Climate Zones Using ArcGIS-Based Method and Exploring Land Surface Temperature Characteristics in Chenzhou, China. *Sustainability* **2020**, *12* (7), 2974. https://doi.org/10.3390/su12072974.
62. Chen, X.; Xu, Y.; Yang, J.; Wu, Z.; Zhu, H. Remote Sensing of Urban Thermal Environments within Local Climate Zones: A Case Study of Two High-Density Subtropical Chinese Cities. Urban Climate 2020, 31, 100568. https://doi.org/10.1016/j.uclim.2019.100568.
63. Zhao, C.; Jensen, J. L. R.; Weng, Q.; Currit, N.; Weaver, R. Use of Local Climate Zones to Investigate Surface Urban Heat Islands in Texas. *GIScience & Remote Sensing* **2020**, *57* (8), 1083–1101. https://doi.org/10.1080/15481603.2020.1843869.
64. Lu, Y.; Yang, J.; Ma, S. Dynamic Changes of Local Climate Zones in the Guangdong–Hong Kong–Macao Greater Bay Area and Their Spatio-Temporal Impacts on the Surface Urban Heat Island Effect between 2005 and 2015. *Sustainability* **2021**, *13* (11), 6374. https://doi.org/10.3390/su13116374.
65. Badaro-Saliba, N.; Adjizian-Gerard, J.; Zaarour, R.; Najjar, G. LCZ Scheme for Assessing Urban Heat Island Intensity in a Complex Urban Area (Beirut, Lebanon). *Urban Climate* **2021**, *37*, 100846. https://doi.org/10.1016/j.uclim.2021.100846.
66. Alghamdi, A. S.; Alzhrani, A. I.; Alanazi, H. H. Local Climate Zones and Thermal Characteristics in Riyadh City, Saudi Arabia. *Remote Sensing* **2021**, *13* (22), 4526. https://doi.org/10.3390/rs13224526.

67. Eldesoky, A. H. M.; Gil, J.; Pont, M. B. The Suitability of the Urban Local Climate Zone Classification Scheme for Surface Temperature Studies in Distinct Macroclimate Regions. *Urban Climate* **2021**, *37*, 100823. https://doi.org/10.1016/j.uclim.2021.100823.
68. Shi, L.; Ling, F.; Foody, G. M.; Yang, Z.; Liu, X.; Du, Y. Seasonal SUHI Analysis Using Local Climate Zone Classification: A Case Study of Wuhan, China. International Journal of Environmental Research and Public Health 2021, 18, 7232. https://doi.org/10.3390/ijerph18147242
69. Stewart, I. D.; Krayenhoff, E. S.; Voogt, J. A.; Lachapelle, J. A.; Allen, M. A.; Broadbent, A. M. Time Evolution of the Surface Urban Heat Island. *Earth's Future* **2021**, *9* (10). https://doi.org/10.1029/2021EF002178.
70. Zhu, R.; Dong, X.; Wong, M. S. Estimation of the Urban Heat Island Effect in a Reformed Urban District: A Scenario-Based Study in Hong Kong. *Sustainability* **2022**, *14* (8), 4409. https://doi.org/10.3390/su14084409.
71. Wang, R.; Wang, M.; Zhang, Z.; Hu, T.; Xing, J.; He, Z.; Liu, X. Geographical Detection of Urban Thermal Environment Based on the Local Climate Zones: A Case Study in Wuhan, China. *Remote Sensing* **2022**, *14* (5), 1067. https://doi.org/10.3390/rs14051067.
72. Wang, Y.; Yao, Y.; Chen, S.; Ni, Z.; Xia, B. Spatiotemporal Evolution of Urban Development and Surface Urban Heat Island in Guangdong-Hong Kong-Macau Greater Bay Area of China from 2013 to 2019. *Resources, Conservation and Recycling* **2022**, *179*, 106063. https://doi.org/10.1016/j.resconrec.2021.106063.